Seventh International Conference on Computational Fluid Dynamics (ICCFD7)
Big Island, Hawaii, July 9-13, 2012

ICCFD7-2004

Numerical Predictions of Sonic Boom Signatures for a Straight Line Segmented Leading Edge Model

A. Elmiligui[1], F. Wilcox[1], S. Cliff[2], and S. Thomas[3]
Corresponding author: alaa.a.elmiligui@nasa.gov

[1] NASA Langley Research Center, Hampton, VA, 23669, USA
[2]NASA Ames Research Center, Moffett Field, CA, 94035, USA
[3]Dell Services Federal Government, Moffett Field, CA, 94035, USA

Abstract: A sonic boom wind tunnel test was conducted on a straight-line segmented leading edge (SLSLE) model in the NASA Langley 4- by 4- Foot Unitary Plan Wind Tunnel (UPWT). The purpose of the test was to determine whether accurate sonic boom measurements could be obtained while continuously moving the SLSLE model past a conical pressure probe. The continuous data acquisition approach allows for accurate signatures approximately 10-15 times faster than a move-pause technique. Two widely used NASA codes, USM3D (Navier-Stokes) and CART3D-AERO (Euler, adjoint-based adaptive mesh), were used to compute off-body sonic boom pressure signatures of the SLSLE model at several altitudes below the model at Mach 2.0. The computed pressure signatures compared well with wind tunnel data. The near field sonic boom signatures were propagated to the ground and the variations in ground signature strength and loudness were evaluated.

Keywords: Numerical Algorithms, CFD, Turbulence Modeling, Supersonic Flows.

Nomenclature

aoa, α	=	angle of attack
CFL	=	Courant-Friedrichs-Lewy number
Cp	=	pressure coefficient
Delx	=	distance between model nose and centerline survey probe orifice, inches
DP	=	overpressure coefficient $(P - P_\infty)$, psf
DP / P	=	overpressure coefficient = $(P - P_\infty) / P_\infty$
H, h	=	altitude, normal distance between the model nose and on-track probe, inches
J	=	Objective function
l, L	=	reference model length, 9.0 inches
M_∞	=	free stream Mach number
MS	=	model station, inches
NF	=	normal force
P	=	static pressure, psf
PM	=	pitching moment
P_∞	=	free-stream static pressure, psf
Re_L	=	Reynolds number based on the model reference length L
SLSLE	=	straight-line segmented leading edge
X	=	streamwise, axial axis
X_{nose}	=	model nose axial location, inches
Y	=	vertical axis
Z	=	spanwise axis

1 Introduction

Over the past 50 years, the primary method used to measure the sonic boom signatures of aircraft in wind tunnels was a single survey probe. Recently pressure rails have been used with varying degrees of success [1]. In a companion paper, an innovative pressure rail, without signature reflection from the surface of the rail or model shock reflection off the wind tunnel wall, is reported to be an accurate and efficient sonic boom measurement technique [2]. A wind tunnel investigation, test 1998, was conducted in October of 2011 in the NASA Langley Research Center (LaRC) 4- by 4-ft Unitary Plan Wind Tunnel (UPWT) to determine the effectiveness of a technique to measure aircraft sonic boom signatures using a stationary conical survey probe while continuously moving the model past the probe. The continuous data acquisition approach allowed for accurate signatures approximately 10-15 times faster than the move-pause technique. The test model for UPWT test 1998 was an existing straight-line segmented leading edge (SLSLE) generic business jet model [3]

The SLSLE model sonic boom signatures were also acquired in LaRC UPWT test 1906 [4], and in NASA Glenn Research Center (GRC) 10- by 10-ft Supersonic Wind Tunnel test D019 [5]. The objectives of test 1906 and D019 were to determine the limiting separation distance between wind-tunnel model and survey probe for the practical extrapolation of pressure signatures from cruise altitude to the ground, and to determine the effect of wing leading edge shape on low-boom performance.

Computational fluid dynamics (CFD) analysis of the sonic boom pressure signatures remains quite challenging [6-13]. Specialized grids that place grid points within the zone of influence of the sonic boom disturbance or solution-adaptive methods are typically applied to obtain accurate off-body solutions. The authors have recently developed and successfully evaluated a Mach cone aligned prismatic cell approach for both inviscid- and viscous-flow computations [7,8]. The mesh is composed of a dense near-field grid with a cylindrically shaped boundary encompassing the model just beyond its surface, and a prismatic mesh from the cylindrical boundary to the far field. The program used to accomplish this is MCAP (Mach Cone Aligned Prism) [7]. The MCAP method maintains the highly refined grid spacing in the axial direction throughout the entire mesh, and allows the user control of the radial stretching and shearing, to align with the Mach cone angle around the aircraft, resulting in accurate on- and off-track signatures.

In the present paper, the effects of viscosity and turbulence modeling on the computed sonic boom signatures of the SLSLE model are evaluated. A sonic boom propagation code sBOOM [14,15] is used to propagate off body pressures and to obtain ground signatures. Numerical simulations are conducted at the aforementioned test conditions, M_∞=2.0, α=2.3°, and Reynolds number of 1.5 million based on body reference length. The CFD codes used in the study were the Unstructured Mesh Three Dimensional (USM3D) [16,17] solver and the Cartesian grid-based Adjoint Error Optimization system (CART3D-AERO) [18,19]. USM3D is a tetrahedral cell-centered, finite volume Euler and Navier-Stokes (N-S) flow solver that was used to provide inviscid, laminar and turbulent flow simulations of the SLSLE model. CART3D-AERO extends the capabilities of NASA's inviscid, embedded-boundary Cartesian mesh solver, CART3D, to include adjoint-based error estimation and automatic mesh refinement. Both codes have been verified and validated over a broad range of problems including supersonic performance and low-boom studies. Comparison of the computed low boom signatures and measured wind tunnel data will be presented and discussed. sBOOM will be used to propagate off body near field pressure signatures and obtain sonic boom ground signatures.

This work was conducted as part of the Supersonic Cruise Efficiency–Airframe element of the NASA Fundamental Aeronautics Program Supersonics Project. The objective of the Supersonic Cruise Efficiency element is to improve aerodynamic design and analysis capabilities for highly efficient, supersonic vehicles. The technical challenges of this element are to develop robust, accurate, and efficient computational methods capable of obtaining sonic boom pressure signatures several body

lengths from a model for rapid design and analysis of supersonic cruise aircraft that are highly efficient and have low sonic boom.

The organization of this paper is as follows: (1) a brief description of the experimental method (wind tunnel model, test and data reduction), (2) description of the CFD codes, USM3D and CART3D-AERO, used in the study, (3) presentation of the numerical results and comparison with wind tunnel data, and (4) Summary.

2 Experimental Methods

The SLSLE model was designed to give the same ground overpressure level as a supersonic business jet concept with a curved leading edge that is produced at a cruise Mach number of 2.0, with a beginning-cruise weight and altitude of 88,500 lbs., and 53,000 feet, respectively. The model was designed to produce a shaped multi-shock ground pressure signature with a bow shock overpressure of 0.5 psf. The SLSLE model was tested in NASA LaRC 4- by 4-ft UPWT (Test 1906) in Sept. 2003, at NASA GRC 10- by 10-ft Supersonic Wind Tunnel (Test D019) in May 2005, and was recently tested in the NASA Langley 4- by 4-ft UPWT (Test 1998) in October 2011. In this section a brief description of the SLSLE model, three wind tunnel tests, and samples of the wind tunnel data are presented.

2.1 SLSLE Model

The SLSLE model is a wing-body configuration with a straight-line segmented leading edge wing, no horizontal or vertical tail, engine nacelles, or canards. A photograph of the SLSLE model is shown in Figure 1. The model leading edge consists of 3 line segments with leading edge breaks at 13.3- and 23.1-percent span. The SLSLE wind tunnel model was rescaled by a factor of 1:160 from the original design scale [4]. The reference length, mean aerodynamic chord, span, and area of SLSLE wind tunnel model are 9 in, 2.9615 in., 4.5 in, and 10.08 in^2, respectively. Figure 2 shows the SLSLE model, sting, and balance reference center locations.

2.2 Wind Tunnel Tests

The sonic boom pressures of the SLSLE model were obtained in three wind tunnel tests. Tests 1906 and 1998 were conducted in the NASA Langley 4- by 4-ft UPWT while test D019, was conducted at the NASA GRC 10- by 10-ft Supersonic Wind Tunnel. In all three wind tunnel tests the sonic boom signatures were obtained at a free-stream Mach number of 2.0 and a Reynolds number of 1.5 million. During a typical sonic boom pressure signature wind tunnel test run, the model was positioned using the tunnel model support system to laterally position it at a specified distance, H, from the survey probe that lies in the model plane of symmetry. Initially, the model was located so that the nose shock was downstream of the survey probe. The model was moved forward in 0.125-inch increments, while the model sonic boom pressure signature data were acquired. A brief description of the wind tunnel tests and model set-ups in the wind tunnels follows.

2.2.1 NASA LaRC 4- by 4-ft UPWT Test 1906

Test 1906 was conducted in 2003 at the NASA LaRC 4- by 4-ft UPWT. The tunnel is a continuous flow, variable pressure, supersonic wind tunnel with two test sections. A complete description of the facility along with test section calibration information is contained in reference [20]. The test was conducted in the low Mach number test section. The test section is approximately 4 feet square and 7 feet long. The nozzle leading into the test section has an asymmetric sliding block that allows for Mach numbers from 1.5 to 2.9. The test was conducted at a Mach number of 2.0.

A schematic drawing of the SLSLE model and pressure probes mounted in the NASA LaRC 4- by 4-foot UPWT tunnel along with a photograph of the model in the tunnel, are shown in Figure 3. A three conical probe survey apparatus was used to measure the pressure signatures. The pressure probes were identical 2° cone angle probes. Data were acquired in a move-pause mode of operation. The probes were mounted to the tunnel sidewall. One probe served as a reference probe and measured the free-stream static pressure and remained in a fixed position. Details of the probes and their installation

can be found in reference [4]. In this paper, only the on-track data from the conical pressure probe under the SLSLE model flight path will be presented, and compared with CFD results. This corresponds to the middle probe on the probe rake . The objectives of test 1906 were to determine the limiting distance (H) between wind-tunnel model and survey probe for the practical extrapolation of pressure signatures to the ground, and the effect of wing leading edge shape on low-boom performance. The reported pressure signatures were for separation distances of 2 to 5 span lengths.

2.2.2 NASA GRC 10- by 10-ft UPWT Test D019

Test D019 was conducted in 2005 at the NASA Glenn 10- by 10-Foot Supersonic Wind Tunnel. The tunnel is a dual-cycle wind tunnel that can operate as a closed-loop (aerodynamic cycle) or open-loop system (propulsion cycle). The tunnel operates at test section speeds of Mach 2.0 to 3.5 and at subsonic Mach numbers below 0.36 [21]. Test D019 was part of the same study as UPWT test 1906. The reported pressure signatures for test D019 was for separation distances of 5 to 20 span lengths. Data were acquired in a move-pause mode. Details of test D019 can be found in reference [5].

A survey apparatus with three conical probes was used to measure pressure signatures in test D019. The probes were mounted to a gust plate that was attached to the tunnel ceiling. A schematic drawing of the SLSLE model and pressure probes mounted in NASA GRC 10- by 10-ft tunnel, along with a photograph of the model in the tunnel, are shown in Figure 4. One probe, mounted to the tunnel sidewall, serving as a reference probe, measured the free-stream static pressure and remained in a fixed position. The reference and survey probes used in the test were the same probes used in UPWT Test 1906. Details of the probes and their installation can be found in reference [5]. In this paper, only the data from the conical pressure probe under the SLSLE model flight path will be presented, and compared with CFD results. This corresponds to survey probe 1 in Figure 4a.

2.2.3 NASA LaRC 4- by 4-ft UPWT Test 1998

The authors conducted test 1998 in 2011 at the NASA LaRC 4- by 4-ft UPWT. Figure 5 shows the general test setup in the UPWT 1998 test. A photograph of the SLSLE model mounted in the test section during UPWT test 1998 is shown in Figure 5c. One of the objectives of test 1998 was to determine the effectiveness of a technique to measure aircraft sonic boom signatures using a single conical survey probe while continuously moving the model past the survey probe. The pressure probes were mounted to the tunnel sidewall. One probe served as a reference probe and measured the free-stream static pressure and one survey probe was used to measure overpressure. A schematic of the probe locations in the tunnel is shown in Figures 5a and 5b. The survey and reference probes were identical 4° included angle cones with two orifices drilled through the probe and into a common chamber that was connected to pressure transducers. To reduce the lag time in measuring the pressure signal, a transducer box was located on the tunnel sidewall above and downstream of the reference and survey probes, as shown in Figure 5. The purpose of the transducer box was to house a differential and an absolute pressure transducer as close to the reference and survey probes as possible.

During this test, sonic boom signatures were obtained using both move-pause and continuous data acquisition methods for comparison. For the continuous sweep runs, the model was positioned so that the nose shock was located downstream of the survey probe. The data acquisition system scan rate for the move-pause runs was 30 samples per second in which data was acquired for two seconds; all of the data acquired during the two-second period were averaged. The data acquisition system scan rate for the continuous runs presented in this paper was 120 samples per second. The axial speed of the model during the continuous runs was approximately 0.09 inches per second. The preliminary data, obtained by the authors from test 1998, are used in the present report for comparison with data from test 1906 test D019 and the computed predictions.

2.3 Wind Tunnel Data

In this section the sonic boom pressure signature measured in tests 1906, D019, and 1998 are compared. This provides a comparison between data acquired in the NASA LaRC 4- by 4-ft UPWT

and the NASA GRC 10- by 10-ft supersonic wind tunnels. Comparisons between data acquired in move pause and continuous mode are also presented. The wind tunnel sonic boom signatures presented in this paper have been adjusted (shifted vertically) so that the value of DP/P (single probe) was nominally zero when the probes were located in the free-stream flow. The procedure used to adjust the pressure signatures consisted of averaging the value of DP/P in the free stream and subtracting the average value from all of the points in that run.

Figure 6 shows a comparison between pressure signatures measured in the LaRC 4- by 4-ft UPWT, test 1906, and at the NASA Glenn 10- by 10-ft Supersonic Wind Tunnel, test D019, at a Mach 2.0 and a separation distance of 5.0 span length (H=22.5 inches) below the model. Delx is the axial distance between the model nose and survey probe and DP/P is equal to $(P - P_\infty) / P_\infty$. The data were acquired in a move-pause mode of operation. Figure 6 shows overall good agreement in the signature length, shock magnitudes, and locations.

Figure 7 shows a comparison of the SLSLE model sonic boom pressure signatures measured in the LaRC 4- by 4-ft UPWT at Mach 2.0 and a separation distance of 3.0 span lengths, H=13.5 inches, below the model for a move-pause mode of operation. Figure 7 shows good agreement between data acquired during test 1906 and test 1998. The discrepancy in the signatures between Delx of 33 and 33.5 inches is due to the differential pressure transducer that was used in test 1998. The transducer was over scaled and had a mechanical stop to prevent transducer damage. Figure 7 also shows good long-term data repeatability between the data collected in tests 1906 and 1998.

Figure 8 shows a comparison of single probe sonic boom signatures, at Mach 2.0 and separation distance of 3.0 span lengths, H=13.5 inches, obtained in move-pause mode, represented by symbols, and continuous mode, represented by solid line, during test 1998. Figure 8 shows overall good agreement in the signature length, overpressure magnitudes, and shock locations. The continuous mode sonic boom signature data exhibits scatter that is, in part, possibly caused by the movement of the model in the tunnel as data is being acquired. The SLSLE model was moving with an approximate speed of 0.09 inches per second. The variation in tunnel flow conditions as a function of location within the test section is another possible factor in the data scatter. One way of smoothing oscillations from the continuous mode data is by applying a moving averaging technique where DP/P for every 201 spatial points is averaged, $\frac{DP}{P}_n = (\sum_{n-100}^{n+100} \frac{DP}{P}_j) / 201$. Figure 9 shows a comparison between averaged continuous data and the data acquired during move-pause mode. The agreement is excellent and proves the validity of acquiring sonic boom signatures by the continuous mode. The time to acquire sonic boom signature in continuous mode was 3.5 minutes compared to the move-pause mode acquisition time of 51.9 minutes. The savings in time and overall good agreement between move-pause mode and continuous mode proves the effectiveness of the technique to measure aircraft sonic boom signatures using a single conical survey probe while continuously moving the model past the probe. The fact that the continuous moving model technique is providing good data implies that data can be acquired with the move-pause technique at significantly greater speeds than in the past.

Figures 6 to 9 show good repeatability between the data acquired in all three wind tunnel tests. In the present study, numerical simulations of the flow around the SLSLE model were conducted for a free-stream Mach number of 2.0, angle of attack of 2.3°, and Reynolds number of 1.5 million based on the model reference length. The computed sonic pressure signatures will be compared with selected data in the subsequent sections of this report.

3 General Description of Computational Methods

Two NASA developed software systems used for the computational analysis were the Tetrahedral Unstructured Software System (TetrUSS) [22] and CART3D-AERO [23] package. NASA LaRC Geometry Laboratory generated the surface grid of the as-built SLSLE model as part of an earlier study [6]. The design angle of attack of 2.3° was built into the surface definition of the model and sting, and hence the angle of attack in the input files of both codes was set to zero. TetrUSS and CART3D-AERO used the same surface mesh. The computational grids, flow solvers, and the boundary conditions for TetrUSS and CART3D-AERO are described below.

3.1 Tetrahedral Unstructured Software System (TetrUSS)

TetrUSS was developed at NASA Langley Research Center and includes: a model/surface grid preparation tool (GridTool), field grid generation software (VGRID, POSTGRID) and a computational flow solver (USM3D). The USM3D flow solver has internal software to calculate forces and moments. Additionally, the NASA LaRC-developed code USMC6 [24] was used for analyzing the solutions.

3.1.1 TetrUSS Computational Grids

USM3D inviscid and viscous volume grids were generated by the Mach Cone Aligned Prism (MCAP) approach [7] for the SLSLE as-built model. A refined unstructured grid within a cylinder in the near field is followed by projection of the surface faces on the cylindrical boundary in the radial direction with a series of prism layers to the far field. The MCAP method maintains highly refined grid spacing in the axial direction throughout the entire mesh, and allows control of the radial stretching and shearing to align tetrahedral cells with the Mach cone angle around the aircraft [7,8]. The inviscid grid consisted of 42 million cells while the viscous grid had 48 million cells. Figure 10 shows the symmetry plane grid colored by pressure coefficient and overlaid constant pressure lines for a USM3D viscous solution of the SLSLE model at Mach 2.0 and α=2.3º. The pressure coefficient is colored white for pressures with Cp value of 0.0, thus the upstream ambient flow grid is not visible. The grid is so dense that the individual triangular faces on the symmetry plane are not visible except for above the model where dense grids are not necessary. The signature sample line at 13.5 inches below the model is shown in red in Figure 10. Proper boundary layer spacing was used to ensure y+ remains less than or equal to 1 for the selected free-stream Mach and Reynolds numbers. It is beneficial to start aligning the mesh as close to the body as possible for accurate sonic boom pressure signatures even at distances less than one body length.

NASA LaRC Geometry Laboratory generated the surface grid of the as built SLSLE model. The scanned data used to generate the as built surface were at a sparse set of locations [10] and evidence of that will show in the results section. Surface patches were created on the configuration in GridTool [25] using the “as built” surface definition, which was generated as part of an earlier study [10]. Sources were placed throughout the domain to cluster cells and accurately capture configuration aerodynamic characteristics. The output from GridTool was used to automatically generate the computational grid domain with the VGRID unstructured grid generation software. VGRID uses an Advancing Layers Method to generate thin layers of unstructured tetrahedral cells in the viscous boundary layer, and an Advancing Front Method to populate the volume mesh in an orderly fashion [27]. POSTGRID was used to close the grid by filling in any gaps that remain from VGRID. POSTGRID is automated to carefully remove a few cells surrounding any gaps in the grid and precisely fill the cavity with the required tetrahedral cells.

The current TetrUSS grids extended up to 30 inches away from aircraft. Authors are currently working with a tool developer to generate a new grid, which extends up to 120 inches below the model. The new grid tool developed by Campbell uses prismatic extrusion approach and is called Boom Grid (BG) [28].

3.1.2 USM3D

The flow solver for the TetrUSS software package is USM3D. USM3D is a tetrahedral cell-centered, finite volume Euler and Navier-Stokes (N-S) method [22]. The USM3D flow solver has a variety of options for solving the flow equations and several turbulence models for closure of the N-S equations [29]. For the current study, Roe’s flux difference splitting scheme was used and CFL_{max} was set to 20. Flux limiters are used within CFD codes to preclude oscillations due to shocks and discontinuities by limiting the values of the spatial derivatives. Typically, a flux limiter is required for supersonic flows and not for subsonic flow computations. For the present study, at the start of a new solution, the USM3D code ran 10000 iterations with first order spatial accuracy, and then the code automatically switched to second order spatial accuracy. Figure 11 shows solution convergence history using Menter’s shear stress transport (SST) turbulence model. The left y-axis is the normalized mean flow residuals and the right y-axis the normalized turbulence model residuals. Details of the

implementation of the SST turbulence model within USM3D can be found in reference [29].

3.2 CART3D-AERO Package

The CART3D-AERO package computes a reliable approximation of user-selected outputs, such as off-body pressure signatures or integrated body forces or moments, through the use of adjoint error estimation and automatic mesh refinement [18]. It allows users to perform automated CFD analysis of complex geometries and is particularly effective in preliminary aerodynamic design.

3.2.1 CART3D-AERO Computational Grids

The computational mesh consists of regular hexahedra everywhere, except for a layer of body-intersecting cells, or cut-cells, adjacent to the boundaries. CART3D-AERO uses adjoint-weighted residual error-estimates to guide automatic mesh adaption. Once a user specifies outputs of interest (lift, drag, etc.) with a corresponding error tolerance, CART3D-AERO automatically refines meshes to drive the remaining numerical errors in the outputs below the requested tolerance [30]. In the current study, the goal was the evaluation of the sonic boom pressure signature. Hence, the function of interest was selected as a pressure coefficient "sensor" along a line in the domain given by:

$$J = \int_0^l \left(\frac{DP}{P} \right)^2 ds \qquad \text{Eq. 1}$$

Figure 12 shows the number of cells at every adaption cycle, as well as the convergence of the pressure integral along the line sensor, the corrected functional, and an estimate of the remaining error on each mesh [19]. The sonic boom signatures were extracted at distances of 13.5, 22.5, 45 and 90 inches below the SLSLE model centerline. For each separation distance, a new simulation was conducted and the line sensor was moved to the corresponding separation distance rather than using multiple sensors in a single computation. Table 1 gives the initial and final cell count for the grids generated by CART3D-AERO.

Table 1. Cell Count For The Various Grids Used In CART3D-AERO Calculation

Distance below Aircraft, h, inches	Initial Mesh cell Count	Final Mesh cell count	Adaption Level
13.5	19,766	16,004,819	10
22.5	253,706	33,638,862	8
45	253,706	34,169,635	8
90	1,228,302	38,901,740	7

3.2.2 CART3D-AERO Flow Solver

A multilevel flow solver is used for all computations with domain-decomposition to achieve very good scalability [23]. The spatial discretization uses a cell-centered, second-order accurate finite volume method with a weak imposition of boundary conditions. The flux-vector splitting approach of van Leer is used in conjunction with the minmod limiter. Convergence to steady state is obtained via a five-stage Runge-Kutta scheme and multi-gridding. CART3D-AERO has also been recently used in the design of supersonic vehicles [11].

3.3 Boundary Conditions

For the inviscid flow simulations, an inviscid aerodynamic surface boundary condition (BC) was used on all solid surfaces. The supersonic inflow BC was used at the domain inflow face and the extrapolation BC was used at the downstream outflow face of the domain. The characteristic inflow and outflow BC was used along the far field, lateral faces of the outer domain. For USM3D viscous simulation the no-slip viscous BC was used on all solid surfaces of the SLSLE model.

3.4 sBOOM

A recently developed NASA sonic boom prediction code, sBOOM, is used to propagate sonic boom signatures to the ground [14]. sBOOM solves the augmented Burgers' equation numerically and takes into account effects such as non-linearity, molecular relaxation and thermo-viscous absorption into the propagation process. The thickness of the shocks is predicted analytically, which avoids artificial smoothing and empirical shock thickening during loudness calculation. sBOOM can predict on-track and off-track ground signatures with or without wind effects, along with consideration for aircraft maneuvers. Further details about sBOOM and its applications can be found in references [14] and [15]. In the present study, computed pressure signatures were propagated to the ground to investigate the variations in ground signatures due to modeling effects and due to initial location of computed near field signature.

4 Results and Discussion

The flow field around the SLSLE model was computed using TetrUSS and CART3D-AERO for free-stream Mach 2.0, α=2.3°, and Reynolds number 1.5 million based on reference length. Conditions were selected to match the experimental data. The SLSLE surface definition had an angle of attack of 2.3º built into the geometry, and hence angle of attack in the input files for both TetrUSS and CART3D-AERO were set to zero. The Sonic boom signatures were extracted at a distance of 13.5, 22.5, 45 and 90 inches below the SLSLE model centerline and compared with wind tunnel data. Sonic boom signatures were propagated to the ground to investigate the effect of inviscid and viscous modeling as well as the separation distance on the ground signature. The flow computations from CART3D-AERO were evaluated at distances of 1.5, 2.5, 5 and 10 body lengths below the SLSLE model. For each separation distance a new simulation was conducted. A line sensor was placed at the separation distance where each of the sonic boom signatures would be extracted. The final grid size and adaption level of all four simulations was given in Table 1.

4.1 CART3D-AERO vs. Experiment

Comparison of the CART3D-AERO computed sonic boom signatures, DP/P, with experimental data, at separation distance of 13.5, 22.5, 45, and 90 inches below the SLSLE model centerline, is shown in Figure 13. The black line is CART3D-AERO results, symbols are the experimental data and the orange line in Figure 13(a) is the LaRC test 1998 continuous mode data. CART3D-AERO results are in good agreement with experimental data in terms of signature length, shock magnitude, and shock locations for all four separation distances. The rate of flow expansion is captured accurately, however the expansion starts later than the test data. CART3D-AERO results match the aft part of the pressure signatures in both expansion and tail shock except at H=90 inches. CART3D-AERO over predicts the magnitude of the nose shock at H=13.5 and 22.5 inches. Figure 14 shows the symmetry plane pressure contours after eight adaptation cycles for a line sensor at H=22.5 inches below the model and a grid size of 33.6 million cells. The refinement pattern shows a relatively fine mesh extending between the model and line sensor, indicating that this region of the flow has a relatively large influence on the pressure signal.

4.2 CART3D-AERO vs. USM3D (Euler) vs. Experiment

The USM3D flow solver was used to obtain inviscid, laminar, and turbulent viscous solutions of the flow around the SLSLE model. The inviscid grid was 44 million cells while the viscous grid was 48 million. The sonic boom signatures were computed at separation distances of H=13.5 and 22.5 inches below model. The USM3D computational grid extended to only 30 inches below model. Comparison of experimental data with USM3D inviscid simulations and CART3D-AERO simulations are shown in Figure 15. There is good agreement between USM3D inviscid results and CART3D-AERO except at the start of the trailing edge expansion, at Delx of 28 inches in Figure 15(a), and Delx of 43.5 inches in Figure 15(b), where USM3D over predicts the pressure signature. Both codes are generally in good agreement with the wind tunnel data, in the forward portion of the pressure signature with a slight discrepancy in the aft region. Although both codes predicted the same expansion rate as the

wind tunnel data, the onset of the expansion was delayed. Other SLSLE model researchers [6,10] reported similar behavior.

4.3 USM3D (Navier-Stokes) vs. Experiment

In an attempt to better capture the onset of the wing expansion, and to investigate the effect of viscous modeling on the prediction of the sonic boom signature, USM3D viscous simulations were conducted. A Navier-Stokes near-field grid was generated using VGRID and then the prism mesh was attached in a similar fashion as the Euler grids. A fully turbulent solution and a laminar solution were obtained. The SST turbulence model was used to model the viscous effects. USM3D laminar sonic boom pressure signatures are compared with experimental data and CART3D-AERO computations in Figure 16. The laminar computation accurately captures the entire signature. The viscous solution matches CART3D-AERO data in the forward part of the signature. The rear portion of the signature now agrees better with experiment. Both laminar and inviscid solutions match the aft part of the expansion wave.

Figure 17 shows streamlines superimposed on lower surface pressure coefficient contours of the SLSLE model. The streamlines show a small change of flow direction near the wing root near the trailing edge. The image shown in Figure 17 is a reflected half-space model, and the upper and lower portions use different initial points for the streamlines. Although flow is predominately laminar and the model was not tripped, the effects of turbulence modeling on the computed sonic boom signature were investigated. Figure 18 shows comparison of USM3D laminar and SST turbulent solution with SLSLE model test data. Both laminar and SST solutions are in good agreement with the experimental data. The SST turbulent solution slightly over predicts the multiple shocks in the wing compression portion of the pressure signature, Delx between 25 and 30 inches in Figure 18(a) and Delx between 41 and 46 inches in Figure 18(b). Overall good agreement of the laminar and SST turbulent solutions is seen. The lack of any evidence of flow separation on the model indicates that the sonic boom signature features are governed by shock structures emanating from the model.

4.4 Extrapolation of Computational Results using sBOOM

The computed near-field sonic boom signatures were propagated to the ground using sBOOM [14]. The signals were scaled up to flight scale before being processed with sBOOM. sBOOM accounts for nonlinearity, molecular relaxation, and thermo-viscous absorption and is capable of off-track propagation given a near-field waveform. Figure 19 shows the ground signatures, DP, versus the signature period for the sonic boom pressure signatures extracted from CART3D-AERO computations, at H/L of 1.5, 2.5, 5.0, and 10.0. The figure shows the sensitivity of the ground signature to the location of the near-field signature to be propagated. The signatures almost coincide except at the peak of the N-wave and at the aft section of the expansion. All four-ground signatures have the same wavelength. The peak of the ground signatures varied by less than 0.05 psf. The corresponding loudness levels are shown in the header of Figure 19. The standard deviation between all 4-ground signatures was 0.65. The sensitivity of the propagated ground signal to the inviscid and viscous modeling is shown in Figure 20. The shape and length of the ground signatures are the same. The peak of the signatures differs by almost 0.015 psf. The standard deviation in the loudness level was 0.6. The small variations in the ground signature and in the loudness levels indicate that the ground signature, as propagated by sBOOM, is insensitive to the type of modeling. Current sBOOM results tend to show that $H/L \geq 1.5$ will provide acceptable ground signature predictions. However this statement is not conclusive, due to the benign nature of the flow around SLSLE model. The H/L distance for acceptable ground signatures may differ for other geometries. For example, geometries with a strong upper surface shock may require additional distance. Further studies involving realistic aircraft configurations need to be conducted and sBOOM predictions validated against flight data.

5 Summary

A sonic boom wind tunnel test was conducted on the SLSLE model in the NASA LaRC 4- by 4-ft. UPWT. The primary purpose of the test was to determine whether the sharp pressure peaks in the sonic boom signature could be measured while moving the model continuously instead of the move/pause mode of operation used in earlier sonic boom tests. The continuous data acquisition

approach allowed for accurate signatures approximately 10-15 times faster than a move-pause technique. The overall good agreement between move-pause mode and continuous mode proved the effectiveness of the technique to measure aircraft sonic boom signatures using a single conical survey probe while continuously moving the model past the probe.

Measured sonic boom signatures were compared with numerical results from two widely used NASA packages, TetrUSS and CART3D-AERO. Numerical simulations were conducted for a free-stream Mach of 2.0, angle of attack of 2.3°, and a Reynolds number of 1.5 million based on the model reference length of 9 inches. The CART3D-AERO package successfully computed the near field sonic boom signature of the SLSLE model. This work proved the ability of the adjoint-based mesh adaptation method to guide refinement and control discretization errors in inviscid simulations. Inviscid, laminar and turbulent solutions were computed with the TetrUSS USM3D flow solver. The Menter SST model was used to model turbulence. The effects of viscous and turbulence modeling on the computed on-track sonic boom signatures were presented. The Mach cone aligned prism cells provided accurate on-track pressure signatures. Dense, stretched, and shock aligned grids are a key parameter in capturing the low boom signature.

sBOOM was used to propagate the computed near field sonic body signatures to the ground. The small variations in the ground signatures and in the loudness levels, generated by SLSLE model, indicate that the ground signature is insensitive to type of inviscid, viscous or turbulent modeling. The loudness level at the ground was about 83 PLdB with a standard deviation of 0.65.

Acknowledgments

The authors would like to thank Norma Farr and Scott Brynildsen of the Geometry Laboratory at NASA Langley Research Center for developing the surface grid. Authors would like to thank Edward Parlette and Sudheer Nayani for developing the volume grids.

References

[1] Durston, D. A., Cliff, S. E., Wayman, T., Merret J., Elmiligui, A., and Bangert, L. Near-Field Sonic Boom Test on Two Low-Boom Configurations Using Multiple Measurement Techniques at NASA Ames. AIAA-2011-3333, 29th AIAA Applied Aerodynamics Conference, Honolulu, Hawaii, June 27-30, 2011.

[2] S. Cliff, A. Elmiligui, M. Aftosmis, S. Thomas, J. Morgenstern, D. Durston: Design and Evaluation of a Pressure Rail for Sonic Boom Measurement in Wind Tunnels. Seventh International Conference on Computational Fluid Dynamics (ICCFD7-2006), Hawaii, July 2012.

[3] Mack, Robert J.: A Supersonic-Cruise Business Jet Concept Designed For Low Sonic Boom. NASA/TM-2003-212435, October 2003.

[4] R. J. Mack and N. S. Kuhn. Determination of Extrapolation Distance With Measured Pressure Signatures From Two Low-Boom Models. NASA/TM-2004-213264.

[5] R. J. Mack and N. S. Kuhn. Determination of Extrapolation Distance With Pressure Signatures Measured at Two to Twenty Span Lengths From Two Low-Boom Models. NASA/TM-2006-214524.

[6] M. B. Carter, and K. A. Deere. Grid Sourcing and Adaptation Study Using Unstructured Grids for Supersonic Boom Prediction," AIAA Paper 2008-6595, 2008.

[7] S. Cliff, A. Elmiligui, R. Campbell, and S. Thomas. Evaluation of Refined Tetrahedral Meshes with Projected, Stretched and Sheared Prism Layers for Sonic Boom Analysis. AIAA Paper 2011-3338, 29th AIAA Applied Aerodynamics Conference, Honolulu, Hawaii, June 27-30, 2011.

[8] Elmiligui, A. A., Cliff, S. E., Aftosmis, M. J., Nemec, M., Parlette, E. B., Wilcox, F. J., and Bangert, L. S. Sonic Boom Computations for a Mach 1.6 Cruise Low Boom Configuration and Comparisons with Wind Tunnel Data. AIAA-2011-3496, 29th AIAA Applied Aerodynamics Conference, Honolulu, Hawaii, June 27-30, 2011.

[9] M. B. Carter, R. Campbell, and S. Nayani. USM3D Analysis of a Low Boom Configuration.

AIAA Paper 2011-3335, 29th AIAA Applied Aerodynamics Conference, Honolulu, Hawaii, June 27-30, 2011.
[10] M. Park. Low Boom Configuration Analysis with FUN3D Adjoint Simulation Framework. AIAA-2011-3337, AIAA 29th AIAA Applied Aerodynamics Conference, Honolulu, Hawaii, June 27-30, 2011.
[11] M J. Aftosmis, M. Nemec and S. Cliff. Adjoint-based low-boom design with Cart3D. AIAA-2011-3500, 29th AIAA Applied Aerodynamics Conference, Honolulu, Hawaii, June 27-30, 2011.
[12] Cliff, S., Thomas, S., McMullen, M., Melton, J., and Durston, D.: "Assessment of Unstructured Euler Methods for Sonic Boom Pressure Signatures Using Grid Refinement and Domain Rotation," NASA/TM-2008-214568, September 2008.
[13] Campbell, R. L., Carter, M. B., Deere, K. A. and Waithe, K. A.: "Efficient Unstructured Grid Adaptation Methods for Sonic Boom Prediction," AIAA 2008-7327, Honolulu HI, August 2008.
[14] S. K. Rallabhandi. "Advanced Sonic Boom Prediction Using Augmented Burger's Equation," AIAA-2011-1278, 49th AIAA Aerospace Sciences Meeting including the New Horizons Forum and Aerospace Exposition, Orlando, Florida, Jan. 4-7, 2011.
[15] I. Ordaz_ and W. Li. Integration of Off-Track Sonic Boom Analysis in Conceptual Design of Supersonic Aircraft. AIAA Paper 2011-464, 49th AIAA Aerospace Sciences Meeting including the New Horizons Forum and Aerospace Exposition, Orlando, Florida, Jan. 4-7, 2011.
[16] Frink, N. T., Pirzadeh, S. Z., Parikh, P. C., Pandya, M. J., and Bhat, M. K.: "The NASA Tetrahedral Unstructured Software System," The Aeronautical Journal, Vol. 104, No. 1040, October 2000, pp. 491-499.
[17] Frink, N. T.: "Assessment of an Unstructured-Grid Method for Predicting 3-D Turbulent Viscous Flows," AIAA Paper-96-0292, January 1996.
[18] Nemec, M., Aftosmis, M. J., Murman, S. M., and Pulliam, T. H.: "Adjoint Formulation for an Embedded-Boundary Cartesian Method," AIAA Paper 2005–0877, Reno, NV, January 2005.
[19] Nemec, M., and Aftosmis, M.: "Adjoint Error-Estimation and Adaptive Refinement for Embedded-Boundary Cartesian Meshes," AIAA Paper 2007-4187, 18th AIAA CFD Conference, Miami FL, June 2007.
[20] C. M. Jackson, W. A. Corlett, and W. J. Monta, W. J.: Description and Calibration of the Langley Unitary Plan Wind Tunnel. NASA TP-1905, 1981.
[21] NASA Glenn web page. http://facilities.grc.nasa.gov/ October 2011.
[22] TetrUSS Web page: http://tetruss.larc.nasa.gov/usm3d/index.html, June 2012.
[23] CART3D Web page: http://people.nas.nasa.gov/~aftosmis/cart3d, June 2012.
[24] Pao, S. P.: "USMC6-TetrUSS Grid and Solution Cutter: A Brief Users' Guide," Version 4, NASA LaRC, September 2010.
[25] Samareh, J.: "GridTool, A Surface Modeling and Grid Generation Tool," Proceedings of the Workshop on Surface Modeling, Grid Generation, and Related Issues in CFD Solutions, NASA CP–3291, May 9–11, 1995.
[26] Pirzadeh, S.: "Unstructured Viscous Grid Generation by Advancing-Layers Method," AIAA Journal, Vol. 32, No. 8, pp. 1735–1737, August 1994.
[27] Pirzadeh, S.: "Structured Background Grids for Generation of Unstructured Grids by Advancing Front Method," AIAA Journal, Vol. 31, No. 2, pp. 257–265, February 1993.
[28] Richard Campbell private communications.
[29] Abdol-Hamid, K. S., Frink, N. T., Deere, K. A., and Pandya, M. J.: "Propulsion Simulations Using Advanced Turbulence Models with the Unstructured-Grid CFD Tool, TetrUSS," AIAA 2004-0714, January 2004.
[30] Nemec, M., Aftosmis, M. J., and Wintzer, M.: "Adjoint-based Adaptive Mesh Refinement for Complex Geometries," AIAA 2008-0725.

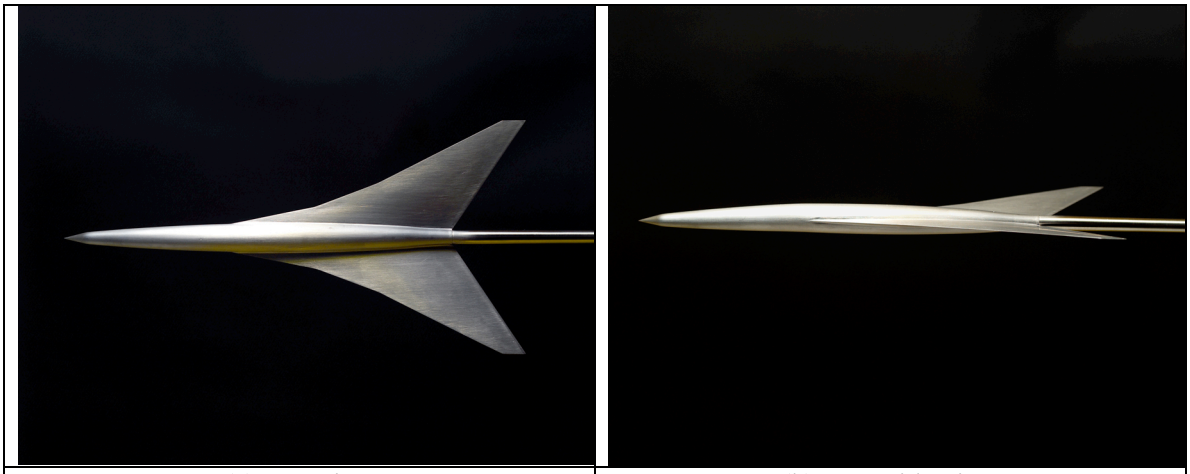

(a) Top view	(b) Near side view

Figure 1: Straight-line segmented leading edge (SLSLE) model.

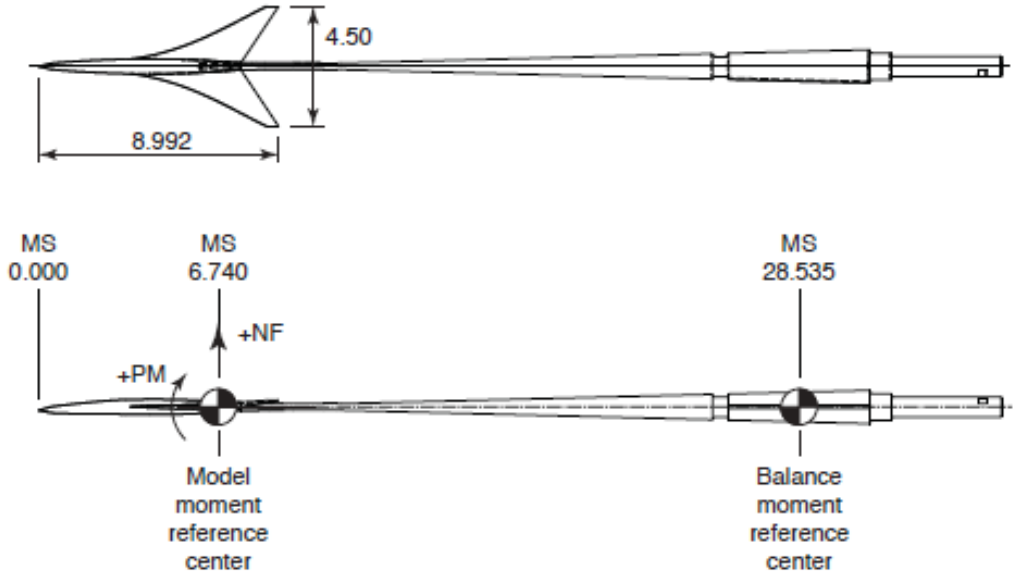

Figure 2: SLSLE model and balance moment reference center locations.
All dimensions are in inches.

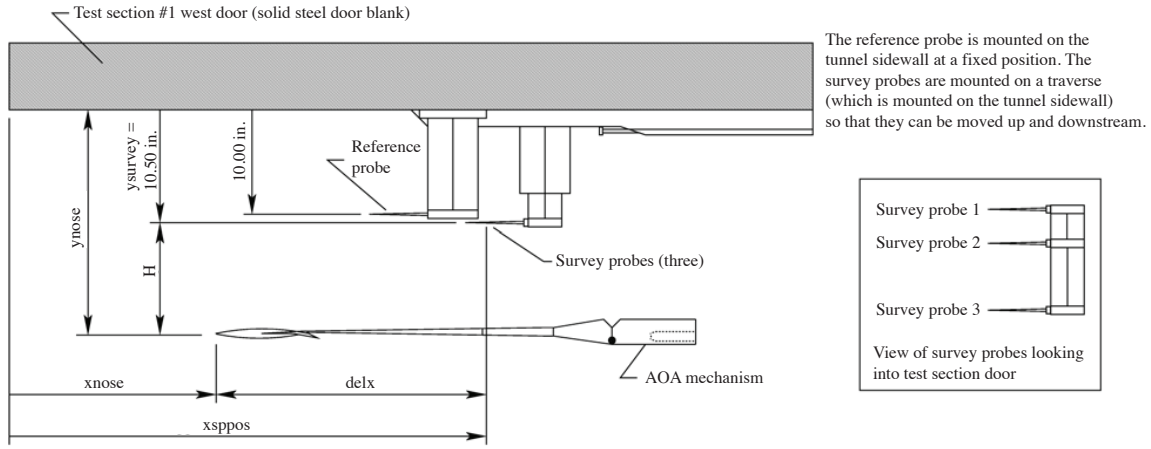

(a) Top view

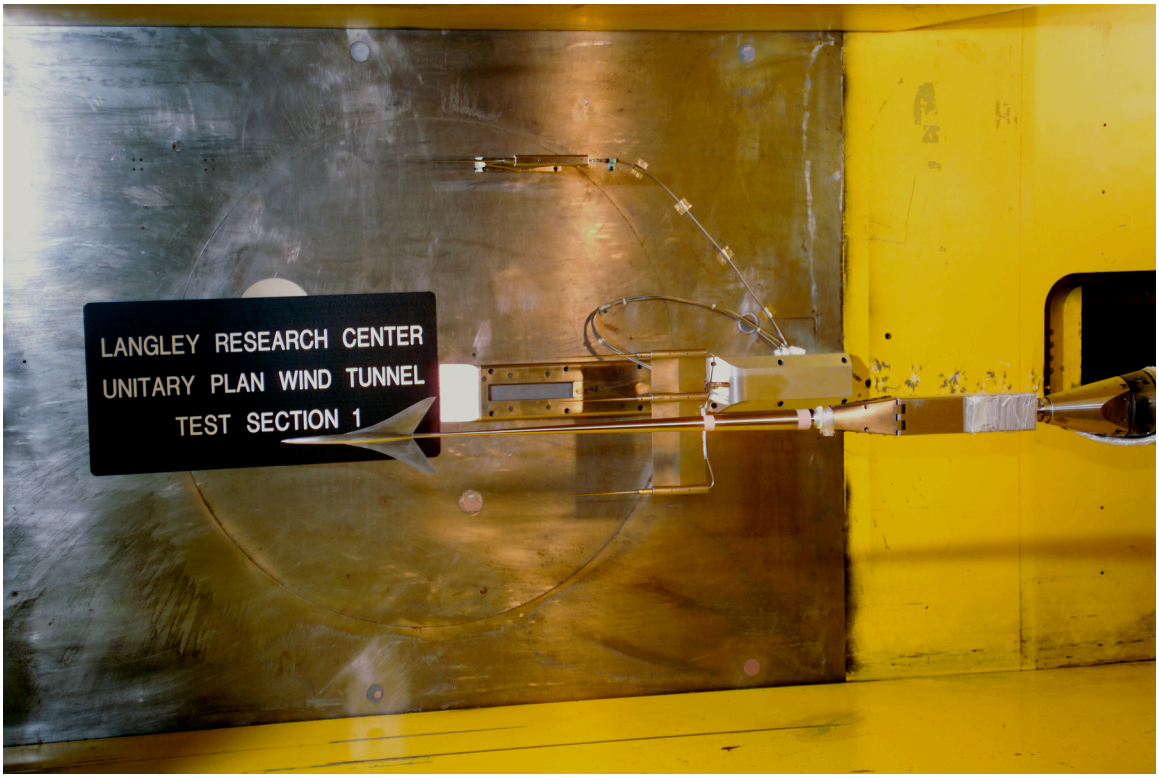

(b) Installation photograph.

Figure 3. Schematic of SLSLE model and the probes used in LaRC UPWT test 1906, Ref. [4].

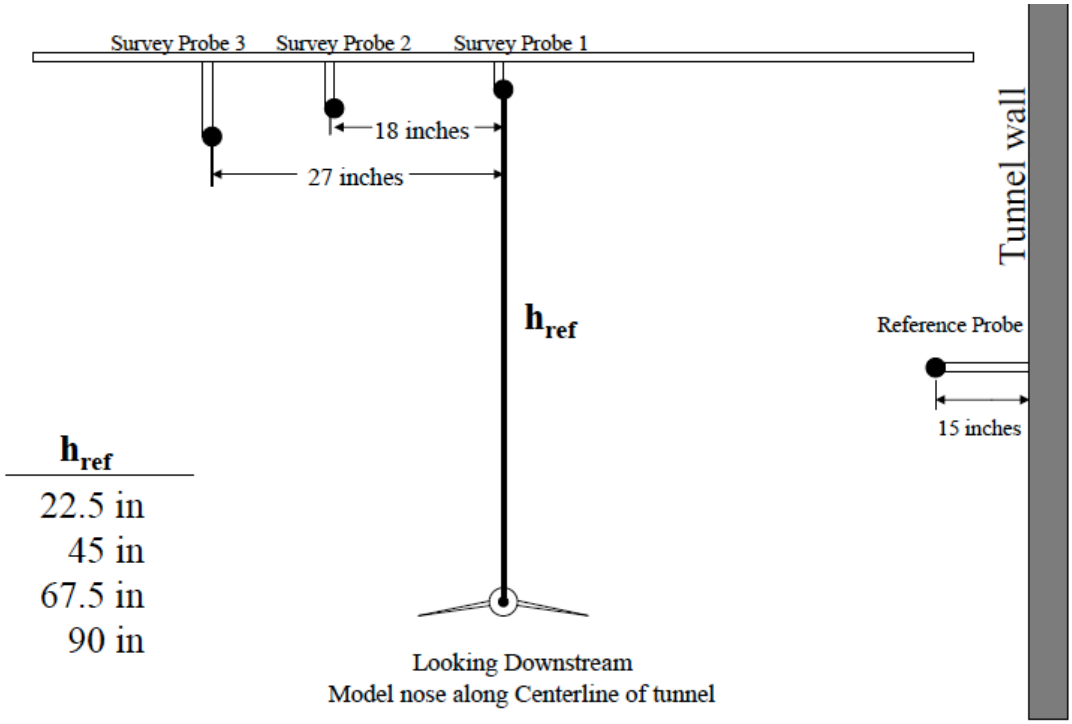

(a) Front View Schematic.

(b) Photograph

Figure 4 SLSLE model and pressure probes in the NASA Glenn 10- by 10- ft tunnel, Ref. [5].

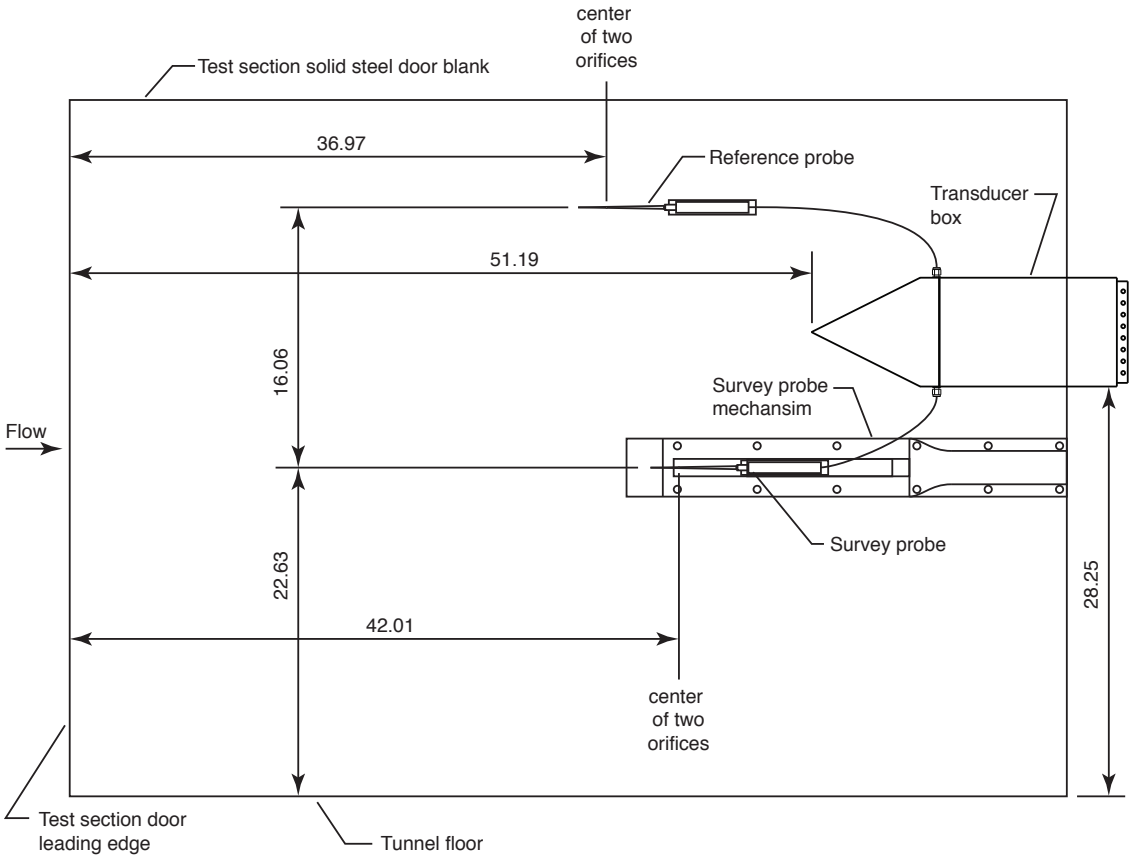

(a) Side view (SLSLE model removed for clarity)

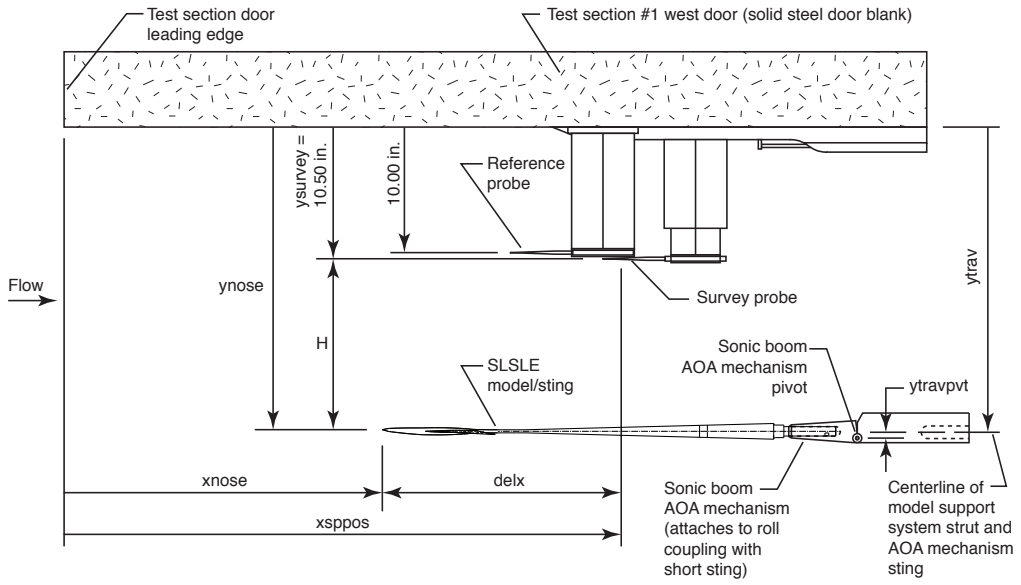

(b) Top view

Figure 5: General test setup for the single conical survey probe in UPWT test 1998. All dimensions are in inches.

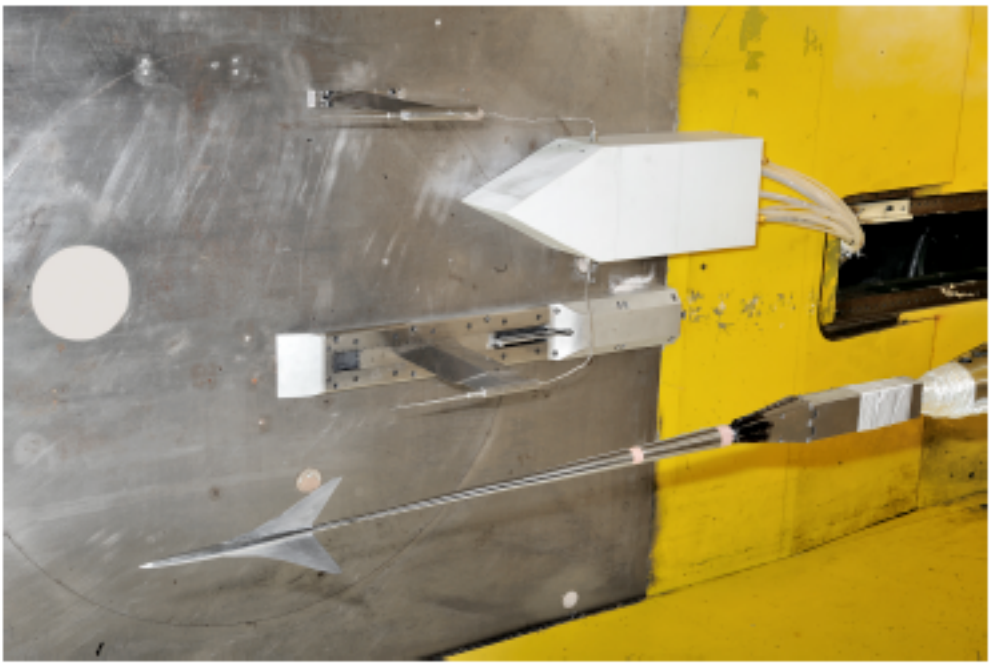

(c) Installation photograph.
Figure 5: Concluded.

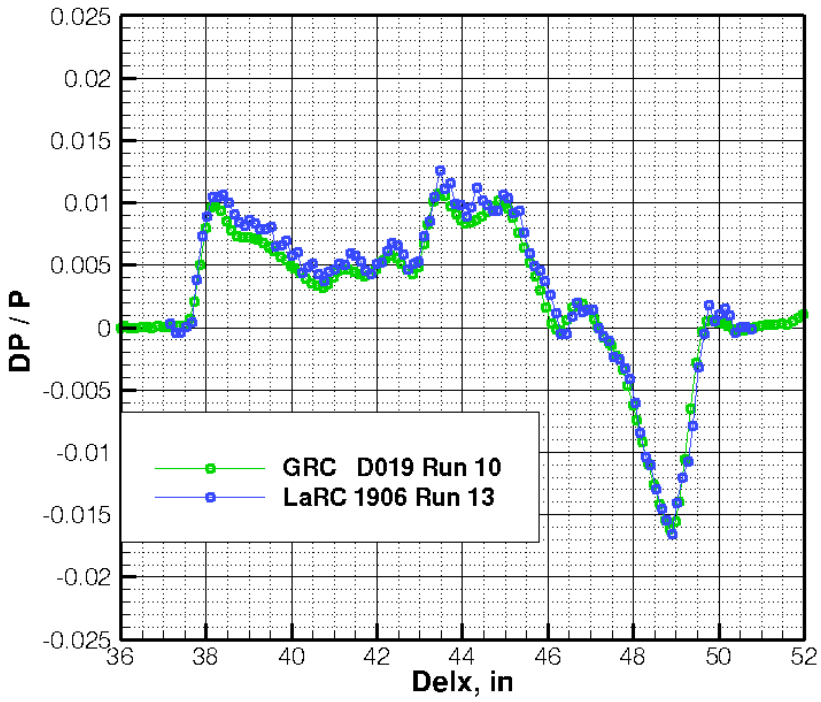

Figure 6: Comparison of SLSLE model sonic boom pressure signatures obtained in move-pause mode. M_∞=2.0, H/L=2.5, H=22.5 inches, Re_L=1.5 million.

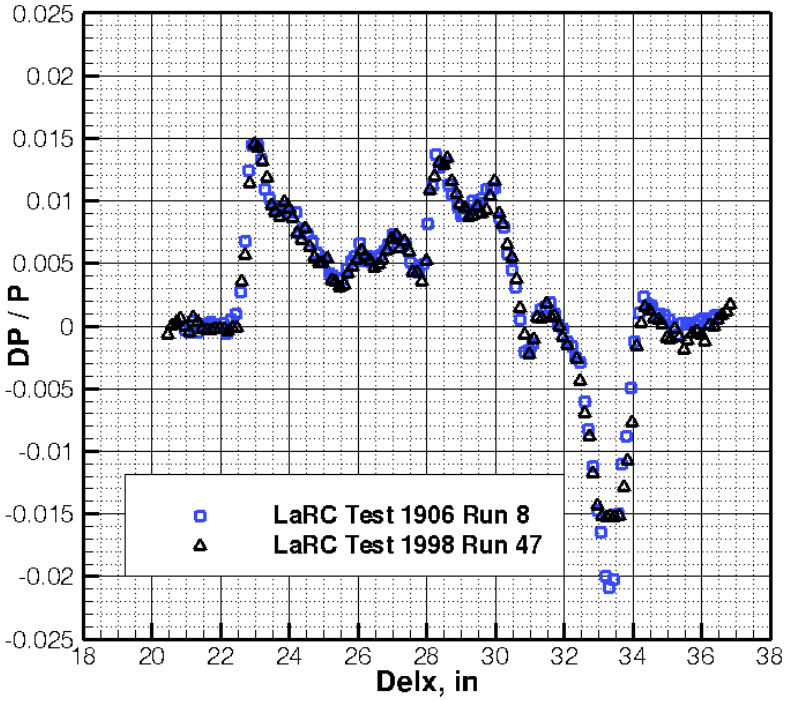

Figure 7: Comparison of SLSLE model sonic boom pressure signatures obtained in move-pause mode. M_∞=2.0, H/L=1.5, H=13.5 inches, Re_L=1.5 million.

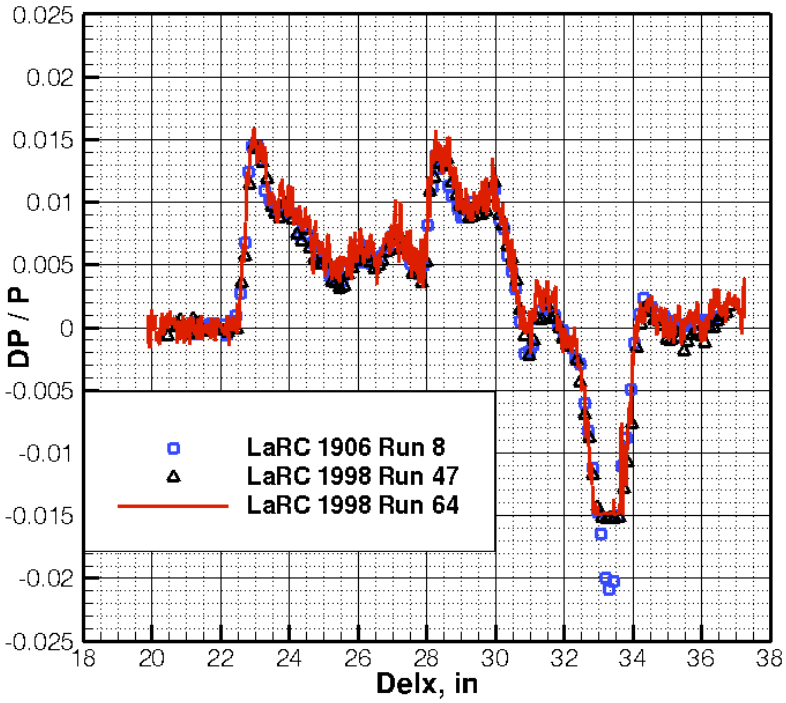

Figure 8: Comparison of SLSLE model sonic boom pressure signatures obtained in move-pause (symbols) and continuous (line) modes. M_∞=2.0, H/L=1.5, H=13.5 inches, Re_L=1.5 million.

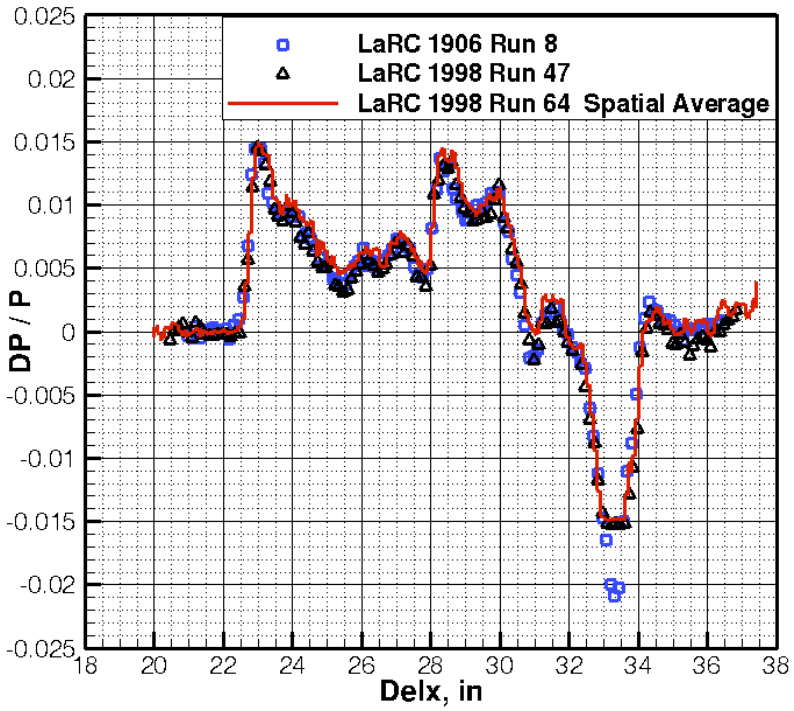

Figure 9: Comparison of SLSLE model sonic boom pressure signatures obtained in move-pause (symbols) and continuous (line) modes. M_∞=2.0, H/L=1.5, H=13.5 inches, Re_L=1.5 million.

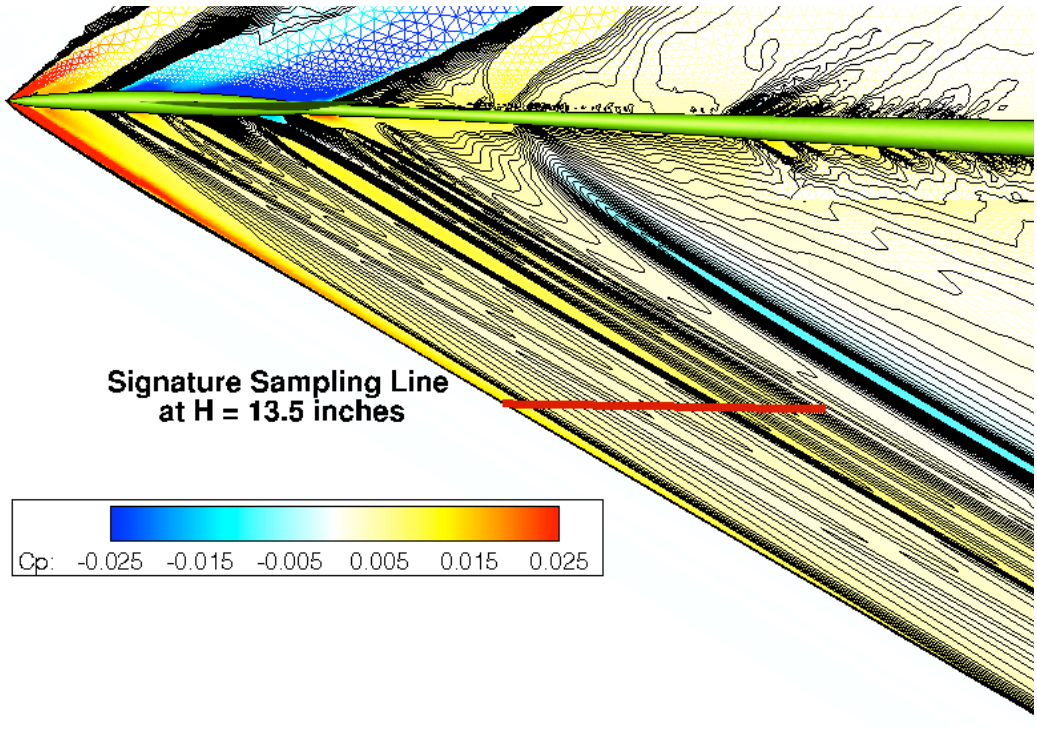

Figure 10: Symmetry plane grid colored by pressure coefficient and overlaid constant pressure lines for USM3D SST solution of the SLSLE configuration, M_∞=2.0, α=2.3°, H/L=1.5, Re_L=1.5 million.

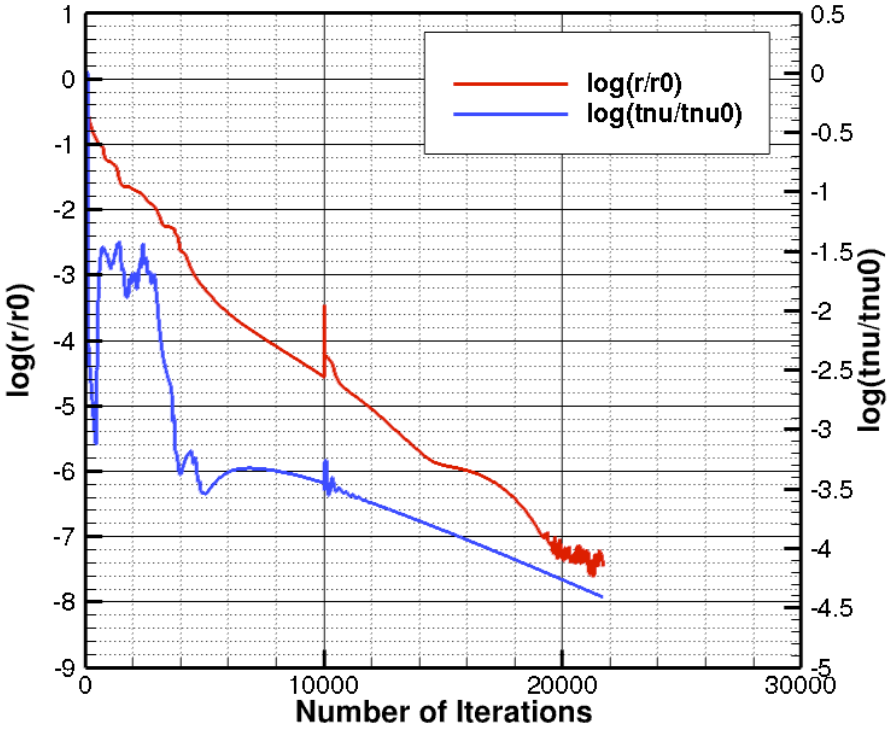

Figure 11: USM3D convergence history.

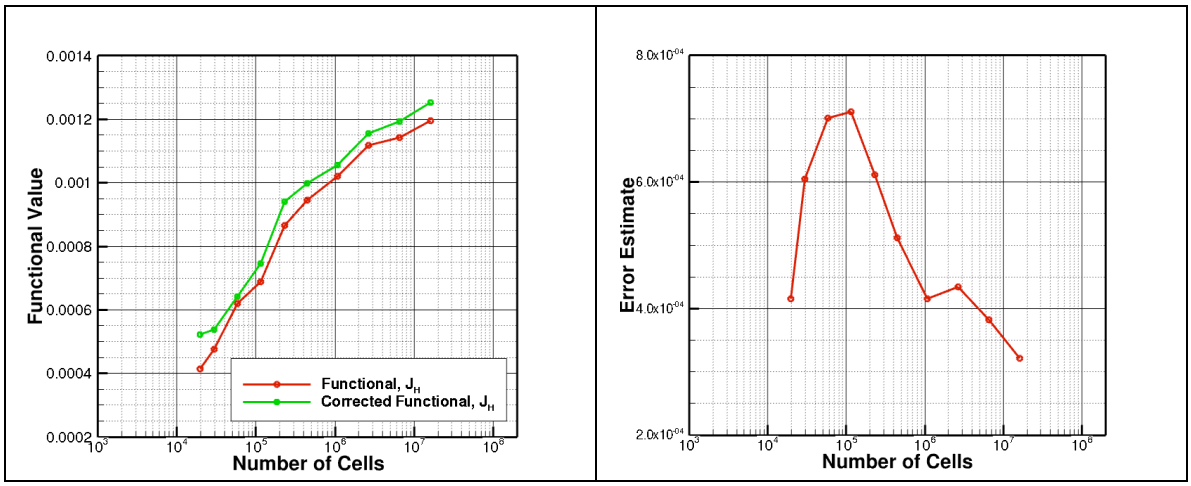

Figure 12: CART3D-AERO mesh convergence of the functional (Eq. 1) and its correction (left), and remaining error estimate (right) for a line sensor at H = 13.5 inches from model.

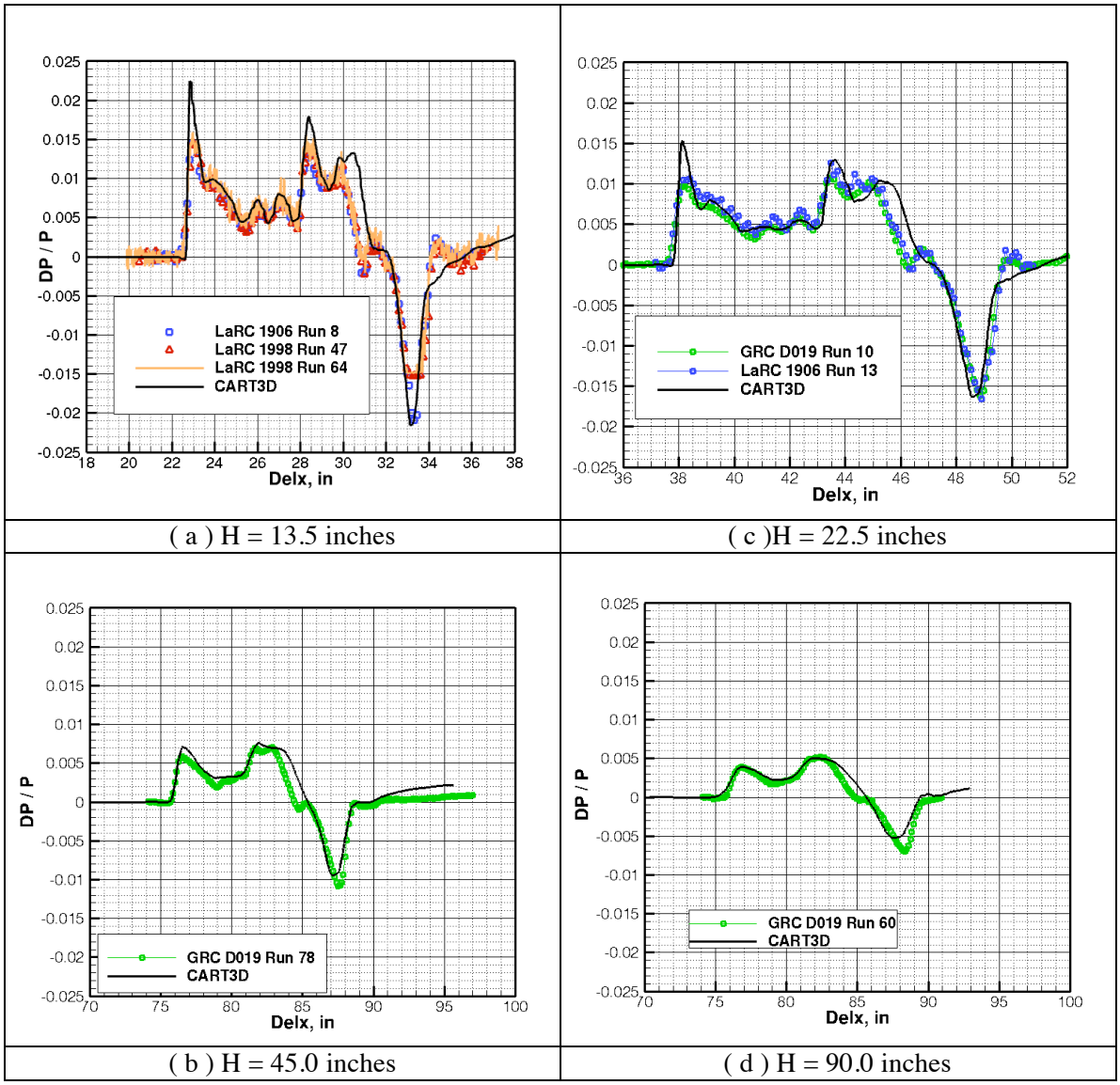

(a) H = 13.5 inches

(c)H = 22.5 inches

(b) H = 45.0 inches

(d) H = 90.0 inches

Figure 13: Comparison of wind tunnel data and CART3D-AERO simulations for SLSLE model. Centerline pressure signatures at various locations below model for M_∞=2.0, α=2.3°.

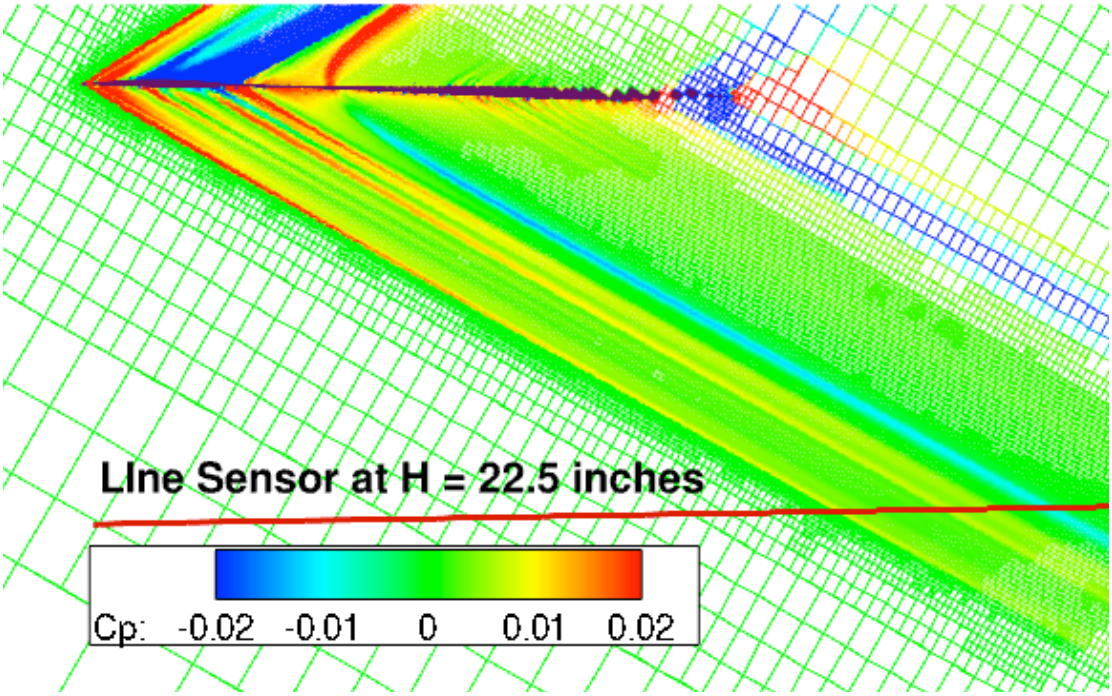

Figure 14: CART3D-AERO simulation of the SLSLE model. M_∞=2.0, α=2.3°, H=22.5 inches.

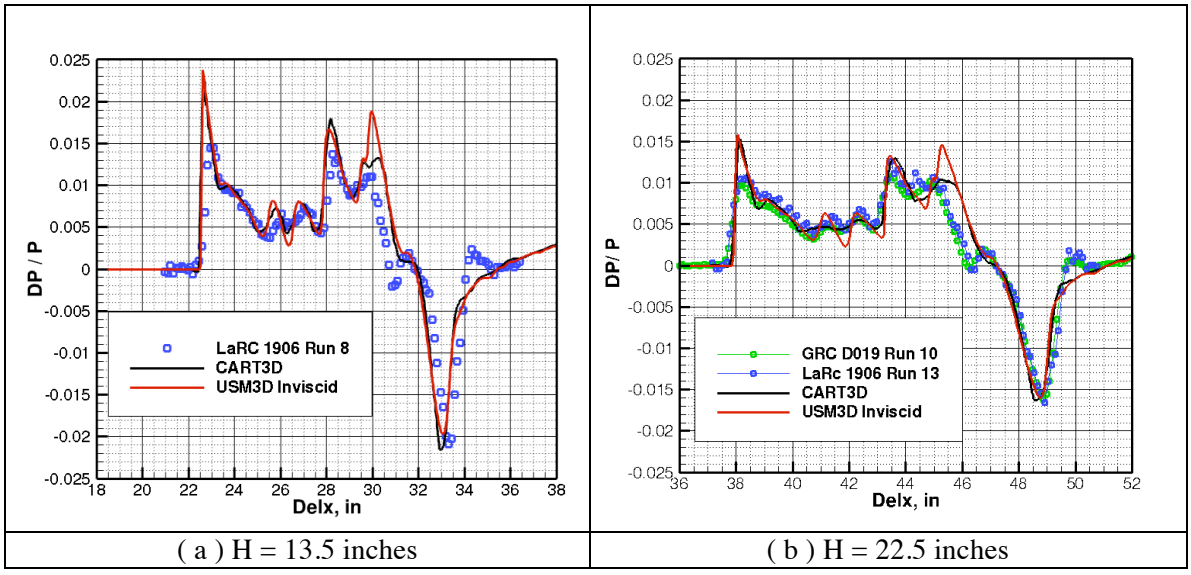

(a) H = 13.5 inches | (b) H = 22.5 inches

Figure 15: Centerline pressure signatures at various locations below model for M_∞=2.0, α=2.3°. Comparison of inviscid USM3D and CART3D-AERO simulations with wind tunnel data.

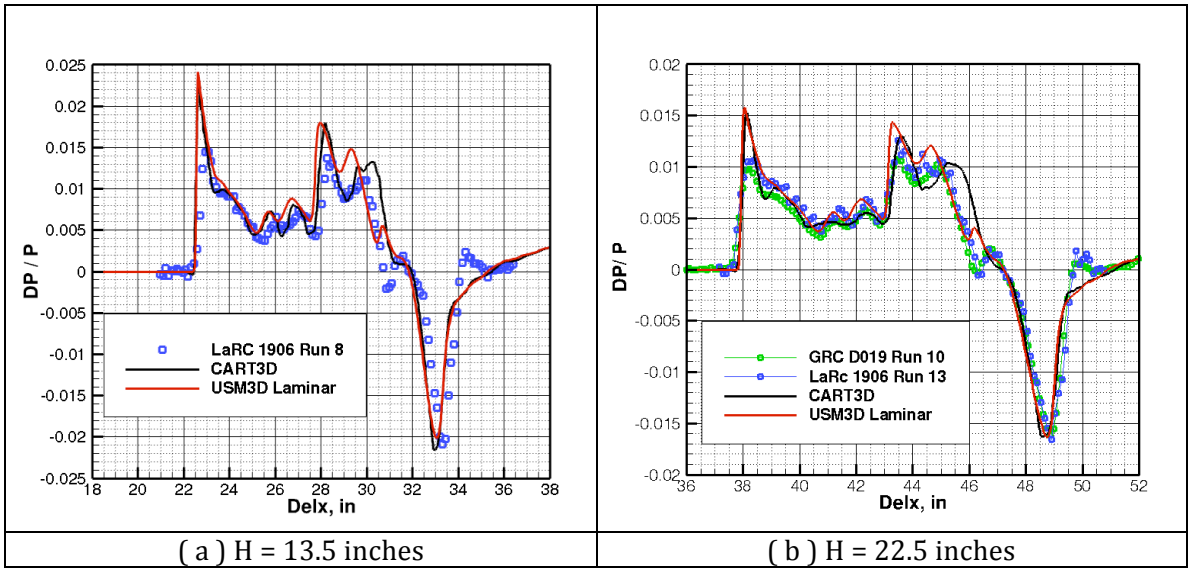

(a) H = 13.5 inches | (b) H = 22.5 inches

Figure 16: Centerline pressure signatures at various locations below model for M_∞=2.0 α=2.3°, Re_L=1.5 million. Comparison of USM3D laminar simulations with wind tunnel data.

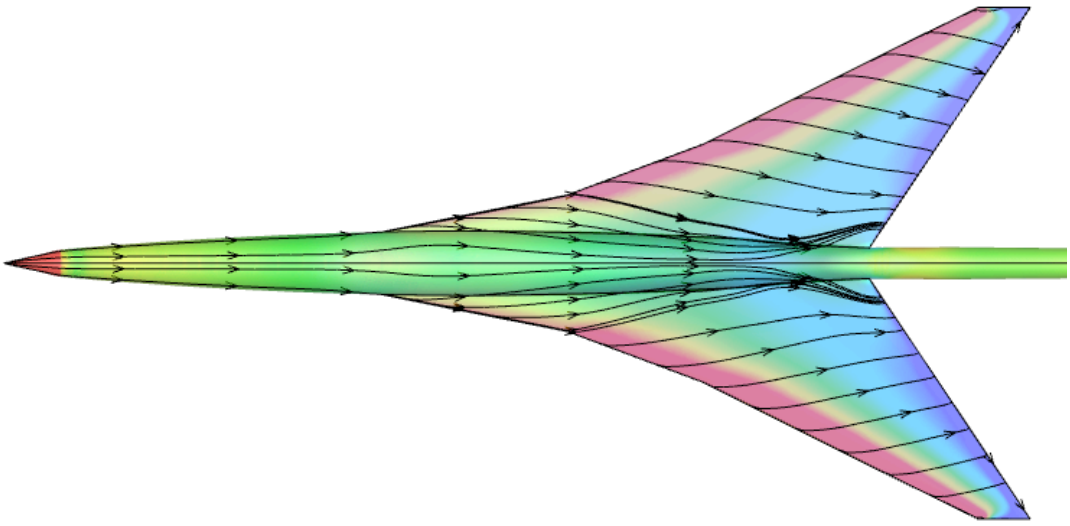

Figures 17: Streamlines superimposed on the lower surface pressure coefficient contours. USM3D laminar solution for M_∞=2.0, α=2.3°, Re_L=1.5 million.

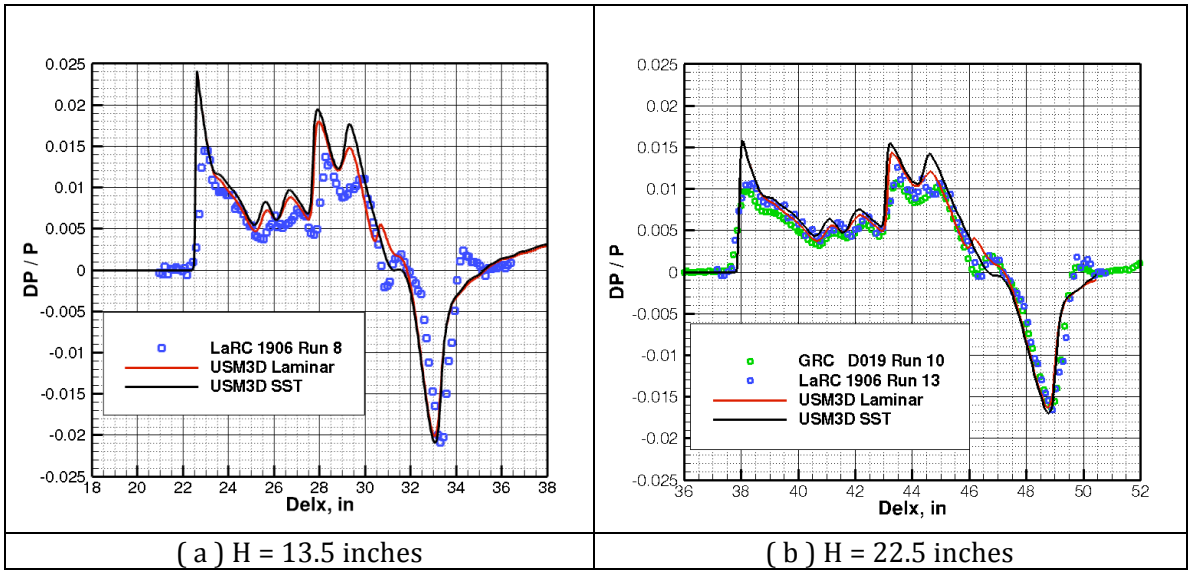

(a) H = 13.5 inches | (b) H = 22.5 inches

Figure 18: Centerline pressure signatures at various locations below model for M_∞=2.0, α=2.3° Re_L=1.5 million. Comparison of USM3D laminar and SST turbulent solutions with wind tunnel data.

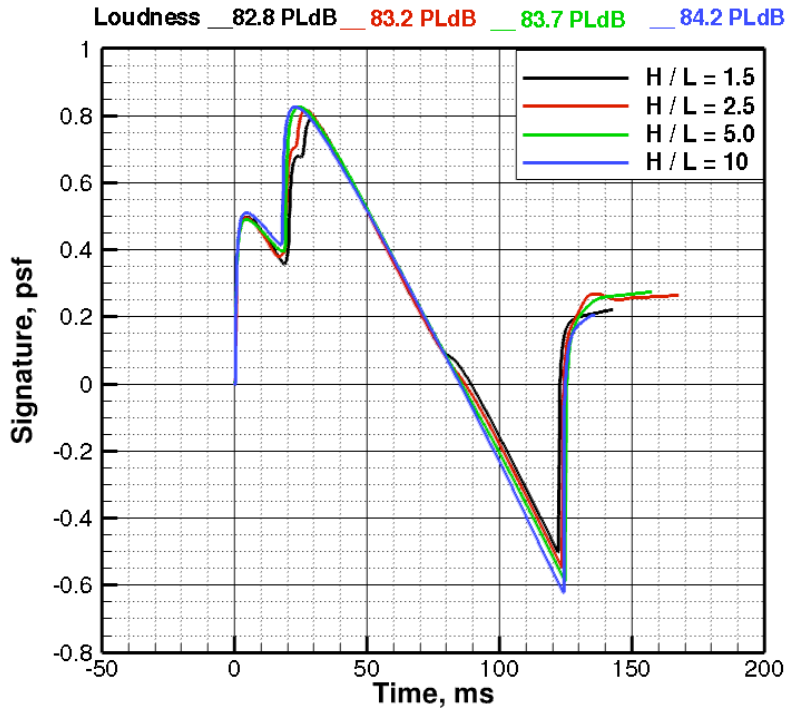

Figure 19: Ground signature sensitivity to separation distance, H/L. CART3D-AERO SLSLE solution, M_∞=2.0.

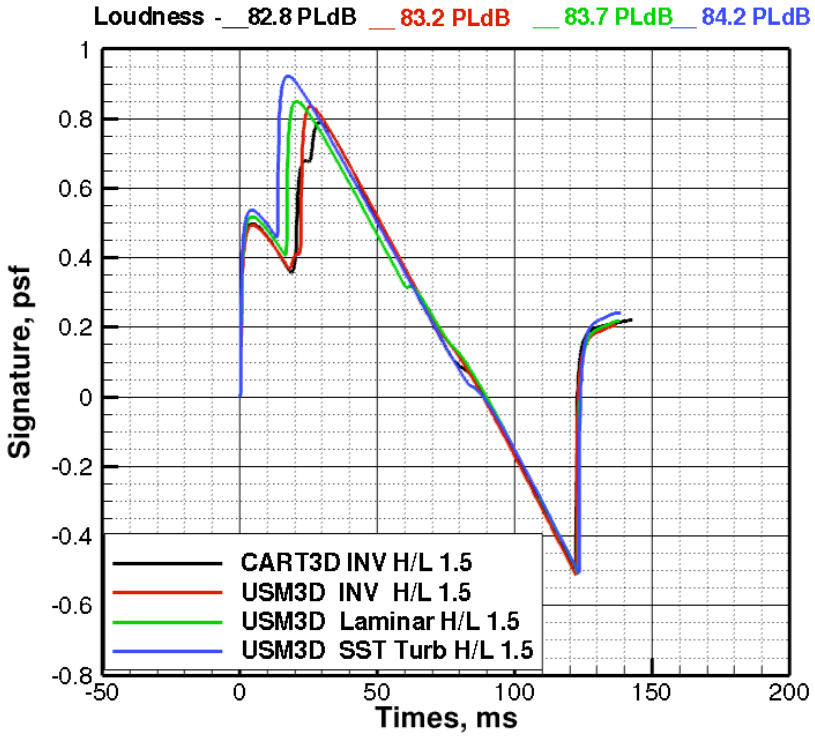

Figure 20: Ground signature sensitivity to inviscid and viscous modeling. M_∞=2.0, H/L = 1.5.